THE JOURNAL OF
PHYSICAL CHEMISTRY

Universitat d'Alacant
Universidad de Alicante

C: Plasmonics; Optical, Magnetic, and Hybrid Materials

Influence of Blending Ratio and Polymer Matrix on the Lasing Properties of Perylenediimide Dyes

Rafael Muñoz-Mármol, Nathalie Zink-Lorre, Jose M. Villalvilla, Pedro G. Boj,
Jose A. Quintana, Carmen Vazquez, Alec Anderson, Michael J. Gordon, Angela
Sastre-Santos, Fernando Fernández-Lázaro, and María Angeles Díaz-García

Just Accepted

ACS Publications

Influence of Blending Ratio and Polymer Matrix on the Lasing Properties of Perylenediimide Dyes

Rafael Muñoz-Mármol,[a] Nathalie Zink-Lorre,[b] José M. Villalvilla,[a] Pedro G. Boj,[c] José A. Quintana,[c] Carmen Vázquez,[c] Alec Anderson,[d] Michael J. Gordon,[d] Angela Sastre-Santos,[b] Fernando Fernández-Lázaro,[b,*] María A. Díaz-García [a,*]

[a] Dpto. Física Aplicada, Instituto Universitario de Materiales de Alicante y Unidad Asociada UA-CSIC, Universidad de Alicante, 03080 Alicante, Spain.

[b] Área de Química Orgánica, Instituto de Bioingeniería, Universidad Miguel Hernández, Elche 03202, Spain.

[c] Dpto. Óptica, Instituto Universitario de Materiales de Alicante y Unidad Asociada UA-CSIC, Universidad de Alicante, 03080 Alicante, Spain.

[d] Department of Chemical Engineering, University of California - Santa Barbara, Santa Barbara, CA 93106-5080, USA.

1
2
3
4
5
6
7
8
9
10
11
12
13
14
15
16
17
18
19
20
21
22
23
24
25
26
27
28
29
30
31
32
33
34
35
36
37
38
39
40
41
42
43
44
45
46
47
48
49
50
51
52
53
54
55
56
57
58
59
60

ABSTRACT

Perylenediimide (PDI) dyes dispersed in polymer films have demonstrated great success as active materials in thin film organic lasers (TFOLs). The type of matrix used to host the dye and the dye doping rate are both crucial parameters to optimize laser performance. This work reports the study of two soluble PDIs, the comercial derivative perylene orange (PDI-O) emitting at around 580 nm , and a new dye (b-PDI-A) with subsituents at the 1,7 bay positions of the PDI core emitting at around 620 nm , dispersed at different doping levels (up to 8 wt% and 50 wt%, for PDI-O and b-PDI-A, respectively) in two widely used polymers for optoelectronics polystyrene (PS) and poly(methyl methacrylate) **(**PMMA**)** . The main goal is to determine which of these two polymers, and at which dye concentration, provides the best results for their use in TFOLs. The assessment of the active materials has been carried out through the analysis of their absorption, photoluminescence and amplified spontaneous emission (ASE) properties. Their capability to form high quality optical waveguides has also been studied by determining gain coefficients and waveguide losses. Results have shown that for both types of PDI derivatives PS is better than PMMA at any concentration, that means larger photoluminescence efficiency, lower ASE thresholds, longer ASE operational lifetimes, larger gain and lower propagation waveguide losses. In addition, the onset concentration at which dye aggregation becomes significant as to negatively affect the optical properties is lower in PMMA than in PS, thus the larger the blending ratio, the larger the superiority of PS with respect to PMMA.

INTRODUCTION

Optically pumped thin film organic lasers (TFOLs) have been investigated for more than a decade.[1,2] Still today, great effort is devoted to the search for high performance materials, that is, with low pump threshold, high efficiency, high photostability, and tunable color emission. Besides, it is also important that the material can be easily processed as a high quality optical waveguide with low propagation losses, by means of solution-based methods.

Inert solid matrixes, among which thermoplastic polymers are the most convenient for thin film processing, serving to host efficient laser dyes dispersed typically at low doping rates (i.e. 1-3 wt%), have shown excellent performances as active materials in TFOLs with distributed feedback (DFB) resonators.[1,3-5] Indeed, thermoplastics, such as polystyrene (PS) or polymethylmethacrylate (PMMA), (see chemical structures in Figure 1) offer several advantages with respect to other materials. They are commercially available, cheap and can be processed in the form of thin films by solution-based techniques such as spin-coating, dip-coating, doctor blading or printing over any substrate.[1] Furthermore, they can be imprinted with relief gratings with techniques such as nanoimprint lithography (NIL), which is very attractive for the fabrication of DFB resonators integrated in the active film itself.[6-9] The matrix plays an important role in the optical and laser performance of the material. Ideally, the matrix should be inert and also provide good dispersion of the dye in order to avoid photoluminescence (PL) quenching and to obtain the maximum possible PL quantum yield (PLQY). Moreover, it should properly isolate the dye and efficiently dissipate heat, which are crucial aspects to avoid photodegradation, and therefore to obtain a long operational durability of the laser device. Many efforts have been devoted to design materials with optimal properties to serve as host matrices for laser dyes used in organic

solid-state lasers (OSLs).[10] This includes a wide variety of organic and inorganic materials, such as glasses, polymers, mesostructured materials, etc., generally prepared in the form of monoliths of several centimetres envisaged to be used with external laser cavities and to be pumped with similar configurations to those used with liquid dye lasers. Some materials have demonstrated great success for such purposes, but often their preparation is complicated and they cannot be processed as good quality optical waveguides, thus limiting their implementation in TFOLs. Interestingly, PMMA (probably the most widely used thermoplastic polymer in optoelectronics) has often been used for OSLs, but less frequently in TFOLs.[4,6,11] The reason for this is PMMA's relatively low refractive index ($n = 1.49$, at $\lambda = 600$ nm), which restricts the selection of an appropriate substrate and film thickness to obtain a low-loss optical waveguide (i.e. with good mode confinement).[4] Actually, there are few studies on the optimization of the matrix, considering not only the emission properties, but also its proccessability as a high quality low-loss optical waveguide.[12,13,14]

With regards to the laser dye, among a wide variety of compounds used, certain highly-efficient soluble perylenediimide (PDI) derivatives have shown great success (dispersed in different types of matrixes) as active materials for both, OSLs and DFBs.[3,4,11,15,16] Up to now, the best performing PDIs for TFOLs have been those with substitutions (needed to provide solubility and therefore film preparation by solution-based methods) at the imide Nitrogen positions of the PDI core. Among them, the one showing the lowest threshold and largest photostability has been the commercial derivative known as perylene orange (PDI-O, see chemical structure in Figure 1).[4,16] DFB lasers based on this dye dispersed in PS have demonstrated applicability for sensors of various kinds.[17-19] In comparison to other dye-doped materials, PDI-O dispersed at 1 wt % in PS has shown very high photostability

(DFB half-life values of 8×10^5 pump pulses, under excitation at two times above threshold with 10 ns pulses at a 10 Hz repetition rate)[3,4,20] and very low thresholds for amplified spontaneous emission (ASE) and DFB lasing (3 kW/cm^2 and 1.7 kW/cm^2, respectively).[4,15] Generally, for most laser dyes, typical doping rates are in the 1-3 wt% range because at higher concentrations, the PL quenches due to molecular interaction and/or the formation of aggregated species. This concentration-dependent PL quenching effect has been the subject of many investigations towards the development of materials with high PLQY at high doping concentrations, or even prepared as neat (undiluted) films or grown as single crystals.[1,2,21] Moreover, this issue reflects the importance of performing concentration-dependent studies when the PL and ASE performance of a given material is to be optimized. [4,5,22-26] The ASE properties of PDI-O dispersed in PS as a function of the dye doping rate (up to 5 wt%) in PS were previously investigated.[4] It was found that the ASE threshold was kept at a low level (below 5 kW/cm^2) up to concentrations of around 3 wt%. The effect of replacing PS by PMMA was also studied, but only at concentrations of 1 wt% and below. It was concluded that within that regime of concentrations, both matrixes behave similarly in terms of photostability and threshold (whenever the film thickness was properly chosen as to obtain a good waveguide mode confinement, that is, ~600 nm and 1000 nm for PS and PMMA, respectively). Within this context, there are several open questions and issues not explored yet, which are important for the optimization of lasers based on PDI-O and PMMA: Is the performance of PMMA similar to that of PS at any dye doping rate? If not, which one is better? Interestingly, in previous work dealing with the optical properties of PDI-O doped PMMA films, it was observed (through changes in the shape of the PL spectrum) that an excimer species formed for dye doping rates of 2 wt% and above.[27] On the other hand, such an excimer is not observed when the matrix is PS

5

instead of PMMA, even up to concentrations of 5 wt%.[4] These interesting and preliminary results suggest that concentration-dependent studies in both PMMA and PS should be carried out, up to the dye solubility limit and/or onset of aggregation and PL quenching. Also important would be to meausure the PLQY for those films. Surprisingly, there is practically no PLQY data in the literature for these materials.[28] It is also worth mentioning that, in spite of the various ASE studies perfomed with PDI-O dispersed in PS, the gain coefficients and the losses, which are also important parameters to describe the performance, have not been previouly determined.

Within the context of designing compounds with proper characteristics to avoid PL quenching as a result of molecular aggregation, an important landmark was a report of a novel PDI derivative (b-PDI-1) that allowed the dye doping rate to be increased ~40 times with respect to previously reported PDIs (up to 27 wt%, limited by the dye solubility in the solvent).[15] At the highest possible concentrations, the films showed ASE emission and rather large PLQY values (~31%), close to values reported in the solid state.[21] Importantly, the b-PDI-1 derivative belongs to a class of PDI derivatives characterized for having substitutions at the bay positions (bay-substituted PDIs, b-PDIs) whose major interest resides in fact on the possibility to expand the range of emission wavelengths of PDIs to values around 620 nm (PDIs substituted at N positions, such us PDI-O, emit always at around 580 nm, independently on the type of substituent). Actually, many efforts have been devoted to designing PDIs emitting at wavelengths longer than 580 nm and showing good laser characteristics. Prior to the report of b-PDI-1, most investigated b-PDIs had shown a rather poor ASE performance because the substitutions at the bay distorted the PDI core, which resulted in a low PL quantum yield and therefore a high threshold and poor photostability.[29,30]

The key aspect of b-PDI-1 was, besides the fact that emits at around 620 nm, its particular chemical structure, with two sterically hindering diphenylphenoxy groups at the 1,7 bay positions , which do not distort the planarity of the PDI core (important to preserve a very high PLQY for the isolated molecule) and, in addition, they induce a molecular conformation that prevents molecular aggregation. Remarkably, there are no studies of b-PDI-1 or other related b-PDIs in other matrixes different than PS. There are just few studies of PMMA used as a matrix for any type of PDI in TFOL devices.[4,11,28] Moreover, important aspects such as the waveguide properties of the films and the effect of the dye doping rate have not been previously analysed. It should be noted that in previous works related to PDI-based TFOLs, PS was the preferred matrix compared to PMMA because of the larger refractive index of the former (values of 1.59 and 1.49, at λ = 600 nm, for PS and PMMA, respectively), which improves the waveguide mode confinement (important to obtain low loss waveguides) and has less limitations for substrate selection.[4,12]

In this work, we perform a systematic study of the optical and ASE properties of waveguide films of both polymers, PS and PMMA, doped with two different PDI dyes, PDI-O and a b-PDI derivative, called b-PDI-A with similar chemical structure (see Figure 1) to that of the previsouly studied b-PDI-1, but with improved solubility. Dye concentration dependence studies, up to 8 wt% for PDI-O, and up to 50 wt% for b-PDI-A, are carried out. The dependence of various properties, such as absorption and PL (at room and low temperature), PLQY, ASE threshold and photostability, and gain coefficients and losses, on dye concentration is analysed and compared for PMMA and PS matrices.
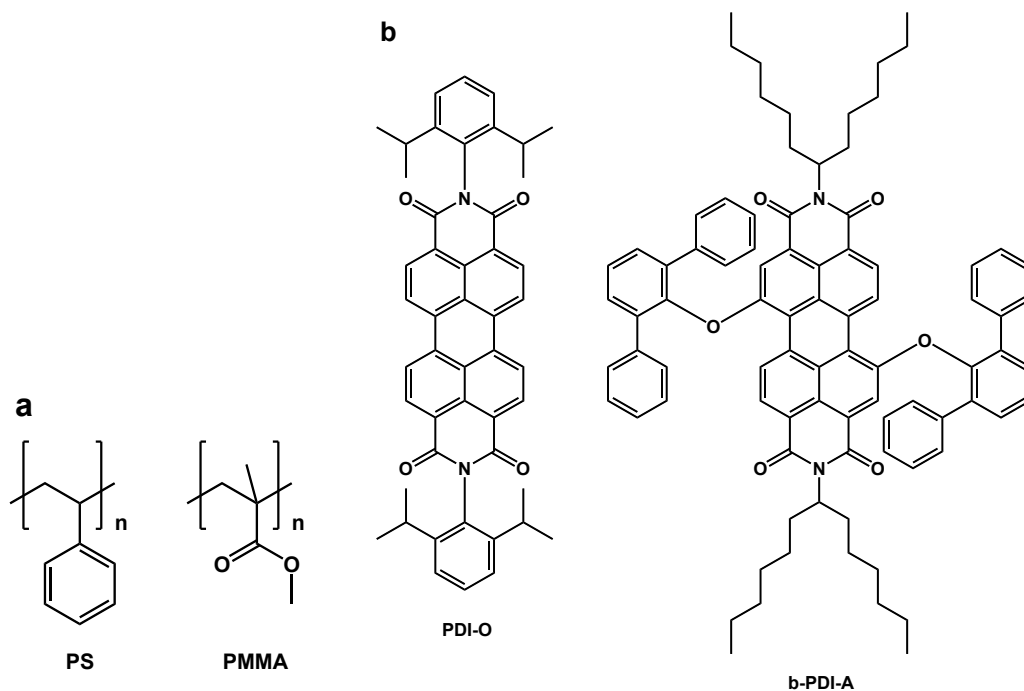
Figure 1. Chemical structures of thermoplastic polymers polystyrene, PS, and poly(methyl methacrylate), PMMA, used as hosting matrixes (a); and perylenediimide, PDI, laser dyes PDI-O and b-PDI-A (b).

EXPERIMENTAL SECTION

Materials

Chemicals were purchased from commercial sources and used without further purification. PS (M = 35000 g mol^{-1}), PMMA (M = 15000 g mol^{-1}), tetrahydrofuran (THF) and dichloromethane (DCM) were purchased from Sigma-Aldrich. PDI-O (M = 711 g mol^{-1}) was purchased from Phiton with a purity higher than 99.5% and b-PDI-A was synthesized following methods previously reported.

Synthesis of *N,N'*-di-(1'-hexylheptyl)-1,7-bis-2,4-diphenylphenoxyperylene-3,4:9,10-tetracarboxydiimide (b-PDI-A)

A mixture of 356 mg (1.45 mmol) of 2,4-diphenylphenol, 281 mg (1.8 mmol) of CsF and 1.95 g (7.4 mmol) of 18-crown-6 were added to a solution of 335 mg (0.37 mmol) of *N,N'*-di-(1'-hexylheptyl)-1,7(6)-dibromoperylene-3,4:9,10-tetracarboxydiimide in dry THF (2 mL). The reaction was refluxed 8 h under argon atmosphere and, after cooling, it was extracted with DCM and washed with water. The organic layer was dried over anhydrous sodium sulfate, filtered and evaporated. Purification was carried out by silica gel column chromatography using CH_2Cl_2:hexane 1:1 as eluent yielding 440 mg (96%) of a pink powder.

^{1}H-NMR (CDCl$_3$) δ 0.85 (t, 12H), 1.25 (br, 32H), 1.82 (m, 4H), 2.18 (m, 4H), 5.09 (m, 2H), 7.02 (m, 10H), 7.39 (m, 10H), 7.74 (m, 6H), 8.37 (br, 2H), 8.58 (br, 2H), 9.20 (d, 2H). ^{13}C-NMR (CDCl$_3$) δ 164.25, 155.01, 147.39, 137.44, 137.36, 136.05, 133.10, 131.23, 131.16, 129.95, 129.34, 128.90, 128.83, 128.61, 128.29, 127.93, 127.86, 127.64, 127.41, 127.35, 126.63, 123.96, 120.68, 54.53, 32.32, 31.78, 29.18, 26.86, 22.58, 14.05. HR-MS MALDI-TOF m/z: [M$^+$] calc. for $C_{86}H_{86}N_2O_6$ 1242.6490, found 1242.6017. IR (KBr): 2925, 2855, 1694, 1655, 1594, 1418, 1405, 1330, 1262, 1186, 754, 699 cm^{-1}. UV-vis (CH$_2$Cl$_2$), λmax/nm (log ε): 478 (3.9), 515 (4.5), 556 (4.7).

Sample preparation

The organic thin films were prepared by the spin-coating technique. Solutions containing the thermoplastic polymer (PS or PMMA) and a varying amount of PDI-O (up to 8 wt% with respect to the polymer) or b-PDI-A (up to around 50 wt% with respect to the polymer), were prepared and cast over SiO$_2$ substrates. After deposition, films were heated (at 90 °C and 150 °C for PS and PMMA, respectively) for 2 hours in order to eliminate the residual solvent. The amount of polymer with respect to the solvent (THF for PDI-O and

DCM for b-PDI-A) was adjusted in order to obtain film thickness (h) of around 600 nm and 1000 nm for PS and PMMA, respectively. Such h values (determined from the fringe pattern of the absorption spectrum)[31] were selected to ensure that the waveguides support only one transversal electric mode (TE_0) which propagates with a high confinement factor, i.e. $\Gamma \sim 90$ % (for details on the calculation of this parameter, see supporting information, section S1) thus minimizing losses and optimizing the ASE performance.[4,12,32,33]

Optical experiments

Absorption and room temperature PL measurements were performed in a Jasco V-650 spectrophotometer and a Jasco FP-6500/6600 fluorimeter, respectively. The absorption coefficient (α) was obtained from the optical density (OD) spectrum using the expression $\alpha = \ln(10)OD/h$. The excitation wavelength used in the PL measurement was 490 nm and 532 nm, for PDI-O and b-PDI-A respectively. The PLQY was measured using an integrating sphere attached to the fluorimeter. For low-temperature PL (LT-PL), samples were cooled to 13 K in a custom-built, closed-cycle helium refrigerator and excited via fiber with 488 or 514 nm light (200-275 mW) from a Coherent I-90 Ar^+ laser. Sample PL was collected using a 0.42NA, 50X long working distance objective and fiber-coupled to a 0.5 m Ebert monochromator with Hamamatsu R928 PMT; the light entering the monochromator was chopped at ~200 Hz and the PMT analog output was synchronously detected using an SRS 830 lockin amplifier. The detection system wavelength sensitivity was calibrated and removed from LT-PL data using a NIST-traceable blackbody source (Ocean Optics LS-1) for reference.

The ASE properties of the films were investigated by optical excitation with a frequency-doubled Nd:YAG laser (10 ns, 10 Hz) operating at 532 nm. Details of the

experimental setup can be found elsewhere.[4,5] Pulse energy was varied using neutral density filters. The pump laser beam was expanded, collimated and only the central part was selected to ensure uniform intensity. A cylindrical lens and an adjustable slit were then used to shape the beam into a stripe of 3.5 mm by 0.5 mm. The stripe was placed right up to the edge of the film, from where PL emission was collected with an Ocean Optics USB2000-UV-VIS fiber spectrometer with 600 grooves/mm grating, giving a spectral resolution of 1.3 nm. The precision in measuring the emission wavelength was around half of this value. The presence of ASE in a given material reflects in the observation of spectral gain narrowing and a sudden increase of the output intensity at a given pump intensity called the ASE threshold. The ASE threshold parameter obtained in the present work refers to the incident pump power density, which is calculated by dividing the incident pump pulse energy by the excitation area over the sample and by the pulse width. The ASE photostability was determined by studying the time evolution of the ASE intensity, while the sample was excited in the same region at constant pump intensity and under ambient conditions. The parameter used to characterize this property has been the same used in previous studies by our group,[3-5] the photostability half-life ($\tau_{1/2}$), defined as the time (or the number of pump pulses) at which the ASE intensity decays to half of its initial value.

For the PDI-O doped films, the gain coefficients at different pump intensities and the propagation waveguide losses, were determined using the variable stripe length (VSL) method.[5,34] We used the same setup as for the ASE characterization, but using an adjustable slit, which enabled changing the excitation stripe length, l, from 0.01 cm to 0.3 cm, the value at which saturation at the intensity output appeared. When ASE is present, the output intensity at the end of the excitation stripe (I) should follow the expression:[34]

$$I(\lambda) = \frac{A(\lambda)I_{\text{pump}}}{g_{net}(\lambda)}\left(e^{g_{net}(\lambda)l} - 1\right) \tag{1}$$

where A is a wavelength (λ) dependent constant, related to the cross section for spontaneous emission; I_{pump} is the pump intensity and g_{net} is the net gain coefficient, which depends on λ, and is related to the gain, g, through $g_{net} = g - k$, where k is a coefficient accounting for the total waveguide loss. The g_{net} coefficient at a given I_{pump} value was determined by fitting the corresponding I versus l curve to equation (1). Then, the loss (i.e. the coefficient k), which is independent of I_{pump}, was obtained by representing g_{net} as a function of I_{pump} and extrapolating the g_{net} value at $I_{\text{pump}} = 0$, at which $g_{net} = -k$.[35]

RESULTS AND DISCUSION

Results are organized in two subsections, related to each of the PDI compounds investigated, PDI-O and b-PDI-A. The various film optical and ASE parameters determined and their dependence on concentration for each of the polymer matrixes used, PS and PMMA, are analysed through Figures 2-4 and Figures 5-7, for PDI-O and b-PDI-A films, respectively. All the relevant parameters for all the films, together with additional secondary information are listed in Table S1 in the Supporting information.

PDI-O dispersed in PS and PMMA films

Optical properties: absorption and photoluminescence

Absorption and PL spectra and PLQY data for PS and PMMA films doped with PDI-O at different concentrations (up to 8 wt%, limited by materials solubility) were obtained for both matrixes. The absorption coefficient increases linearly with dye concentration and the absorption spectral shape remains unaltered (see Figure S2, supporting information). No

significant differences are found between PS and PMMA, except for a 3 nm difference in the peak wavelengths. On the other hand, important features are observed in the PL spectra (Figure 2a), which have been normalized by dividing by the film optical density at the excitation wavelength, to facilitate comparison. For both matrixes, the spectral shape changes significantly and the PLQY decreases as the doping rate increases (see Figure 2b). Both features are signs of aggregation and excimer formation.[27,36,37] Remarkably, for the PMMA films, the spectral changes start appearing at concentrations of around 2.5 wt%; this value is much lower than that observed for PS (~ 5 wt%), indicating that PDI-O has better dispersion in PS. This is also in accordance with the PLQY values, which are higher in PS than in PMMA at each concentration.

The observation of PDI-O excimers in PMMA at concentrations of 2.5 wt% and its negative effect on the PL efficacy, was previously reported,[27] although in that work, ASE and PLQY data were not provided. In fact, PLQY data for PDI-O in PMMA have been scarcely reported.[28]

Low temperature photoluminescence (LT-PL, 13K) measurements of PDI-O in both PMMA and PS matrices at blending ratios of 1, 2.5 and 8 wt% are shown in Figure S3 (see Supplementary Information). For the lowest blending ratio (1 wt%) in both polymers, PDI-O PL emission has molecule-like character, with a clear 00, 01, and 02 vibronic progression $[S_0 \rightarrow S_1(v=0,1,2)]$ of the π-π* transition, indicative of isolated chromophores. However, as blending ratio increases, PMMA is seen to more quickly disrupt the 00/01 vibronic progression compared to PS, suggesting that the onset of aggregation occurs more easily in PMMA. The latter is echoed in both, the room temperature PL and the quicker falloff of PLQY for PMMA. The striking similarity of RT and LT-PL results, namely the well-

resolved vibronic progression, is indicative that non-radiative losses associated with scattering with lattice phonons and/or thermally activated emission from excitons above the bottom of the $S_1(v=0)$ band are not significant,[38] in contrast to many other systems.[39] In addition, the lower 00/01 vibronic peak ratio at low temperature may indicate that aggregates may act in a more ordered fashion, as the 00 transition is forbidden in a perfectly ordered H-aggregate.[40]
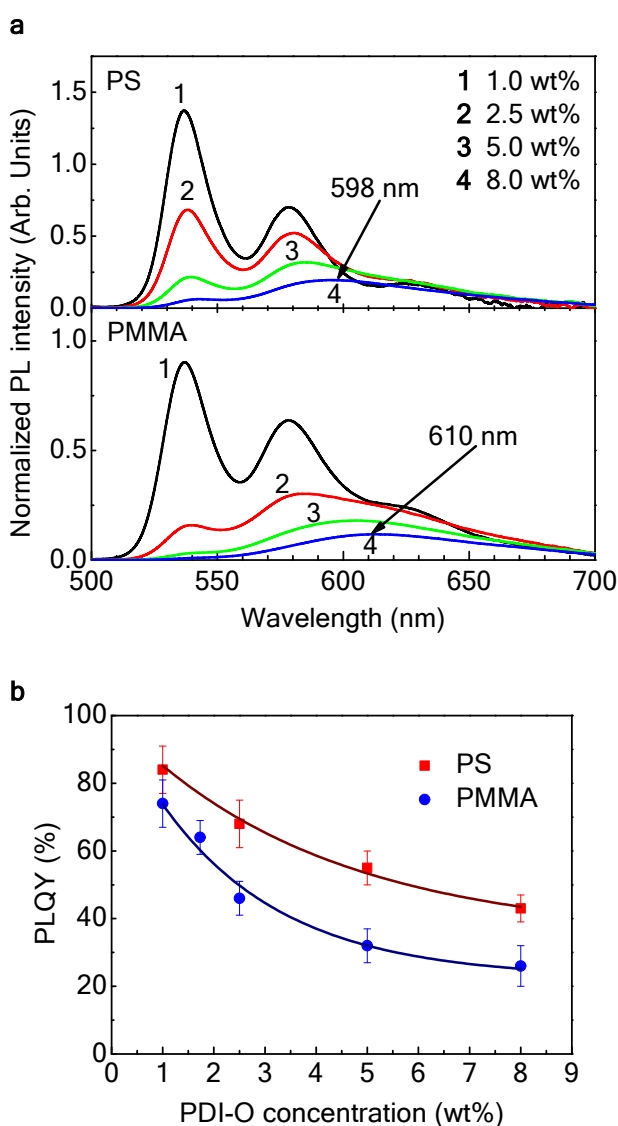

Figure 2. Photoluminescence properties of PDI-O dispersed in PS and PMMA films.

(a) Normalized photoluminescence (PL) intensity, i.e. PL intensity divided by the optical

density at the excitation wavelength, both versus wavelength for PDI-O dispersed at various doping rates in PS and PMMA films (top and bottom of the panels, respectively). Labels 1, 2, 3 and 4 in the figures correspond to dye concentrations of 1, 2.5,5 and 8 wt%, equivalent to 1.4, 3.6, 7.5 and 12.3 ($\times$ 10^{-5} mol/g). The wavelength of the maximum intensity peak for the film with highest doping rate is indicated next to its corresponding spectrum; (b) PL quantum yield (PLQY) versus dye concentration for PDI-O dispersed in either PS (squares) or PMMA (circles). Full lines are guides to the eye.

ASE properties: spectra, thresholds and operational lifetimes

The ASE properties of the films were investigated for all the films. ASE emission appears at around 580 nm, close to the first vibrational PL peak, as illustrated in Figure 3a, in which ASE spectra for various PS and PMMA films are shown, particularly for low and high concentrations (the highest for each polymer at which ASE is observed).

The ASE threshold, $I_{\text{th-ASE}}$, for each film was determined from the plot of the emission linewidth (defined as the full width at half of the maximum intensity, FWHM) versus the pump intensity, I_{pump} (see illustrative example in Figure S4 in the Supplementary Information), as the I_{pump} value at which the FWHM decreases to half of its initial value and approximately coincident with a sudden increase in emission intensity. $I_{\text{th-ASE}}$ values for all the films which show ASE are represented in Figure 3b as a function of the dye concentration in the films. For the PS films, results are in agreement with previous measurements:[4] the lowest $I_{\text{th-ASE}}$ values (3 kW/cm^2) are obtained for concentrations between 1 wt% and 3 wt%; for higher concentrations $I_{\text{th-ASE}}$ increases rapidly. For the PMMA films, the lowest $I_{\text{th-ASE}}$ value (12 kW/cm^2) is also obtained at a low concentration

(1 wt%) and gets larger as the concentration increases, although in this case, the increase in $I_{\text{th-ASE}}$ occurs at lower concentrations. Remarkably, at a given concentration, $I_{\text{th-ASE}}$ for PS is in all cases lower than for PMMA, and the difference is larger at high concentrations. The observed detriment on the ASE performance is attributed to the formation of a PDI-O-based excimer species.[23,27,36,37]

The ASE photostability of PDI-O at concentrations of ≤ 1 wt% in PS and PMMA has been previously studied.[4] Within that concentration regime, these materials show very long ASE half-lives (of the order of 10^5 pump pulses, with I_{pump} two times above threshold) and no significant differences were found between PS and PMMA. In the present work, we performed experiments at higher concentrations and found, as expected,[5,15] a decrease of the ASE half-life as the doping rate increases (see data in Table S1, supporting information). For the range of concentrations at which no aggregation occurs, and thresholds are low (up to 3 wt% in PS), the decrease in lifetime is simply due to more photobleaching because the film absorbs more light. On the other hand, for higher concentrations, at which the threshold increases due to the formation of excimers, the half-life decreases more rapidly, mainly because the I_{pump} needed to obtain ASE is larger and the lifetime is highly dependent on the I_{pump} used. [3,20] With regards to highly doped PMMA films, the photostability is significantly worse, in accordance with the fact that excimer formation appears at lower concentrations than in PS.
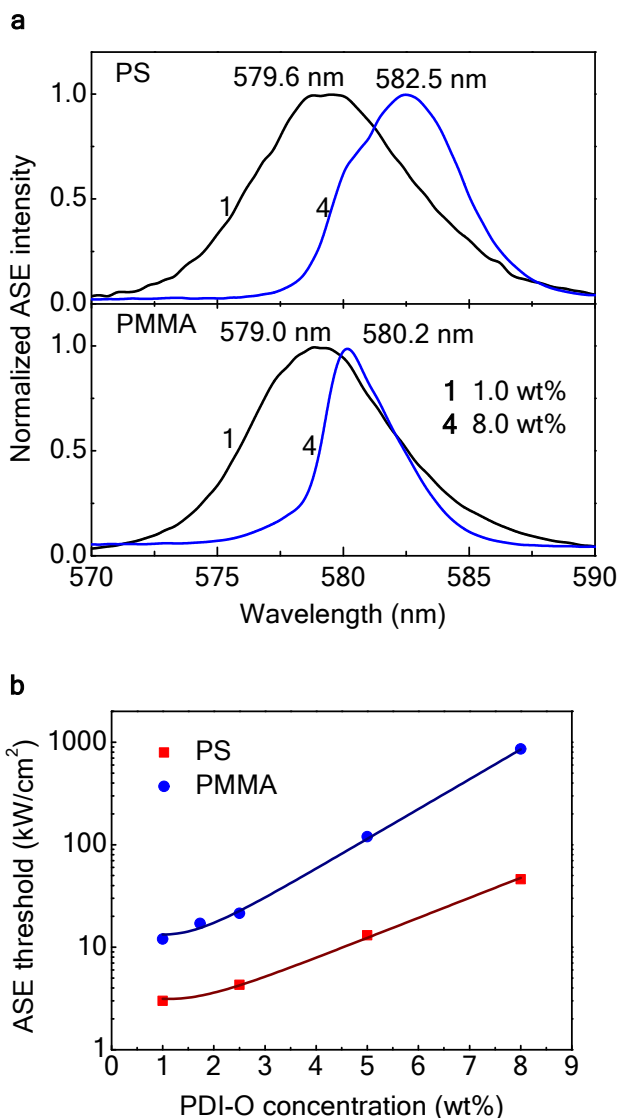
a

b

Figure 3. Amplified spontaneous emission (ASE) properties of PDI-O dispersed in PS and PMMA films. (a) Normalized ASE spectra, i.e. ASE intensity divided by its maximum value for PS and PMMA films (top and bottom of the panel, respectively) doped with PDI-O at concentrations of 1 and 8 wt% (labels 1 and 4, respectively); (b) ASE threshold as a function of dye concentration for PS (squares) and PMMA (circles) films doped with PDI-O. The full lines are guides to the eye.

Gain coefficients and propagation losses

17

Net gain coefficients (g_{net}) were determined by fitting to equation (1), as explained in the experimental section, data from plots of the output intensity versus the excitation length, at a given I_{pump}. Examples of such plots are shown in Figure S5 of the Supplementary information. The g_{net} values obtained at different I_{pump} values are represented in Figures 4a and 4b for PS and PMMA films, respectively, at two dye concentrations (1 and 5 wt%)

For the 1 wt% PDI-O-doped PS film, a g_{net} value of 38.8 cm^{-1} at I_{pump} = 14.6 kW/cm^2 was obtained. Remarkably, this value is higher than that of other PDI derivatives (g_{net} = 2 cm^{-1}, at $I_{pump.}$ = 26 kW/cm^2)[23] and comparable to values obtained with other state-of-the-art dye-doped polymers, i.e. g_{net} of 60 and 6 cm^{-1} at I_{pump} of 43.3 and 11.5 kW/cm^2, respectively, for a carbon-bridged oligo(*p*-phenylenevinylene) derivative dispersed at 8 wt% in PS.[5] The 1 wt% PDI-O doped PMMA film also shows a rather large gain (g_{net} = 26.8 cm^{-1}, at $I_{pump.}$ = 19.9 kW/cm^2), although somewhat inferior to that obtained with PS. This is in accordance with the ASE threshold, which is a bit higher in PMMA. On the other hand, the differences between PS and PMMA are very significant at high dye doping rates (much larger gain with PS), also in accordance with the ASE threshold results.

The plots of g_{net} as a function of I_{pump} (Figures 4a and 4b) were used to determine the loss (k), which is independent of I_{pump}, by extrapolating the g_{net} to I_{pump} = 0. As observed, at low dye concentration (1 wt%), k of the PS film (6 ± 1 cm^{-1}) is around half of that of the PMMA film (15 ± 3 cm^{-1}). This might explain the slightly higher ASE threshold of the latter. On the other hand, at high dye concentration (5 wt%), the PS film shows a value (k = 8 ± 1 cm^{-1}), similar to that obtained at low concentration, while the PMMA one shows a value almost two times larger (25 ± 3 cm^{-1}) than the one at low concentration. The fact that the loss for the PS film is the same for both concentrations indicates that film optical

quality is similar, which means that the dispersion of PDI-O in the film is good. It is also

indicative that the observed increase in the ASE threshold (Figure 3b), and the decrease in

the net gain coefficient (Figure 4a) when increasing dye concentration from 1 wt% to 5

wt%, is not because of an increase in k. Thus, the apparent existence of molecular

aggregation (evidenced by excimer formation) which is responsible for the observed PLQY

decrease and which negatively affects the threshold and gain performance, does not

apparently affect the optical film quality. On the other hand, in the case of PMMA, results

seem to indicate that the formation of the excimer not only affects the PLQY, but also film
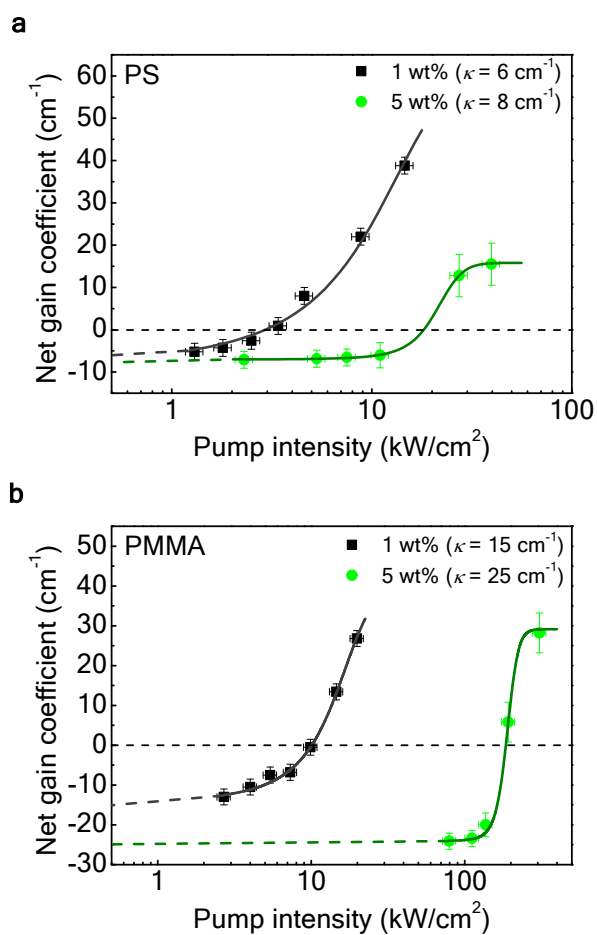
optical quality.

Figure 4. Net gain and loss coefficients of PDI-O dispersed in PS and PMMA films. Net gain coefficient versus the pump intensity for PDI-O dispersed in PS and PMMA films (a and b, respectively) for dye concentrations of 1 and 5 wt% (circles and squares, respectively). Full lines are guides to the eye and their intersection with the Y axis correspond to the loss coefficient, *k* (values in legend).

b-PDI-A dispersed in PS and PMMA films

Synthesis of b-PDI-A

The synthesis of the b-PDI-A derivative has been carried out for the first time in almost quantitative yield by substitution of the dibromoperylene derivative with diphenylphenol in the presence of CsF and 18-crown-6, using our previously described method (Scheme 1).[41] b-PDI-A was characterized by standard techniques such as ^{1}H-NMR, ^{13}C-NMR (See Figure S6 in the Supporting Information) and UV-vis spectroscopies, and high resolution MALDI-TOF spectrometry.
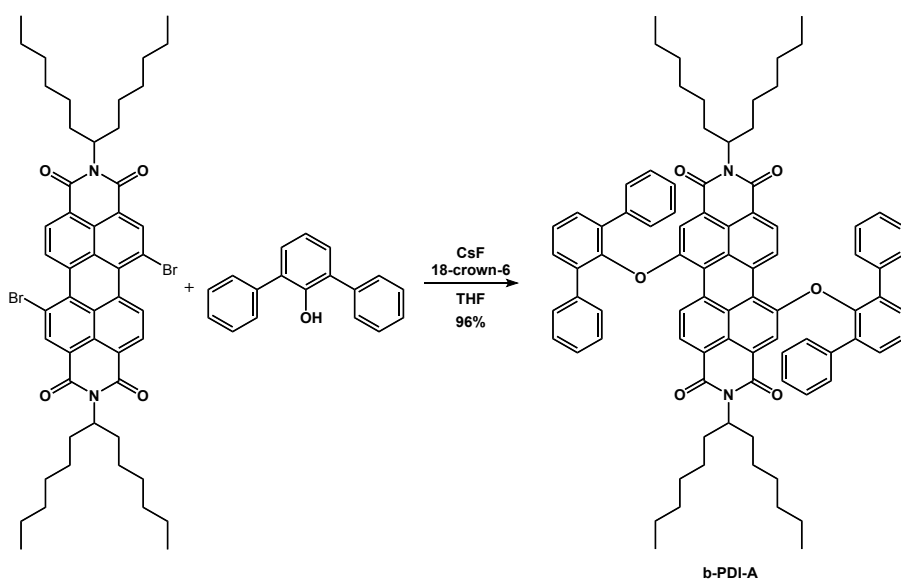
b-PDI-A

Scheme 1. Synthesis of b-PDI-A.

Optical properties of films: absorption and photoluminescence

Absorption and PL spectra and PLQY data for PS and PMMA films doped with b-PDI-A at different concentrations were obtained. Absorption and PL spectra are significantly red-shifted with respect to those of PDI-O (see Figure S7 in Supporting information and Figure 5a, respectively). This is a consequence of the presence in b-PDI-A of electron-rich substituents in the bay positions of the PDI core. It should also be noted that in this case, the range of dye concentrations in the film (up to around 47 wt%) is much larger than those explored in section 3.1 for PDI-O (up to 8 wt%), mainly because aggregation occurs at larger concentrations as discussed in detail below. It should also be remarked that b-PDI-A has very good solvent solubility to prepare films of proper thickness. This fact is the reason why the concentration range used now is larger than the one explored in a previous work with a similar b-PDI derivative (called b-PDI-1) dispersed in PS (in that case the maximum concentration was 27 wt%).[15] The b-PDI-A compound used here has longer aliphatic chains attached to the N positions than those of b-PDI-1, which provide the improved solubility.

The general behavior of the absorption properties as a function of dye concentration is similar to that observed with PDI-O. For both matrixes, the absorption coefficient increases linearly with dye concentration and the absorption spectral shape is practically unaltered (see Figure S7, supporting information), except for a slight red shift from the film with the lowest concentration to the one with the highest one (1 nm and 4 nm in the PS and PMMA films, respectively). No significant differences are found between PS and PMMA, except for the peak wavelengths which are slightly lower in PMMA (4 nm for the film with lowest concentration and only 1 nm with the one with highest concentration).

With regards to the PL properties, in contrast to PDI-O, the spectral shape does not change significantly (Figure 5a) when concentration increases. No additional peaks, such as the one observed with PDI-O at long wavelengths above certain concentrations, and ascribed to the existence of an excimer species, can be seen in this case. As expected, the PL peaks red-shift when the concentration increases. Importantly, the PL efficiency clearly decreases with concentration (see PLQY data in Figure 5b), indicative of some kind of aggregation or molecular interaction. Similar to PDI-O, the PL efficiency is better in PS than in PMMA for b-PDI-A. Moreover, it is seen that in PS, the PL quenching effect becomes more significant for concentrations above 10 wt%, while in PMMA, this occurs above 5 wt%. These results indicate, as in the case of PDI-O, that for this b-PDI-A derivative, the dispersion in the matrix is better in PS than in PMMA. LT-PL measurements in Figure S8 (Supplementary Information) also clearly demonstrate that the 00, 01, 02 vibronic progression for b-PDI-A is well maintained at high blending fractions (up to 47 wt%) in PS, but a shift from 00 to 01 preferentially occurs in PMMA between 10 and 47 wt%. Moreover, the similar PL spectra for b-PDI-A in PS, up to very high blending ratio as compared to PDI-O, demonstrate the efficacy of functionalizing the PDI core at the 1,7 bay positions with diphenylphenoxy groups significantly disrupt molecular packing, aggregation, and/or crystallization, which would otherwise lead to PL quenching.
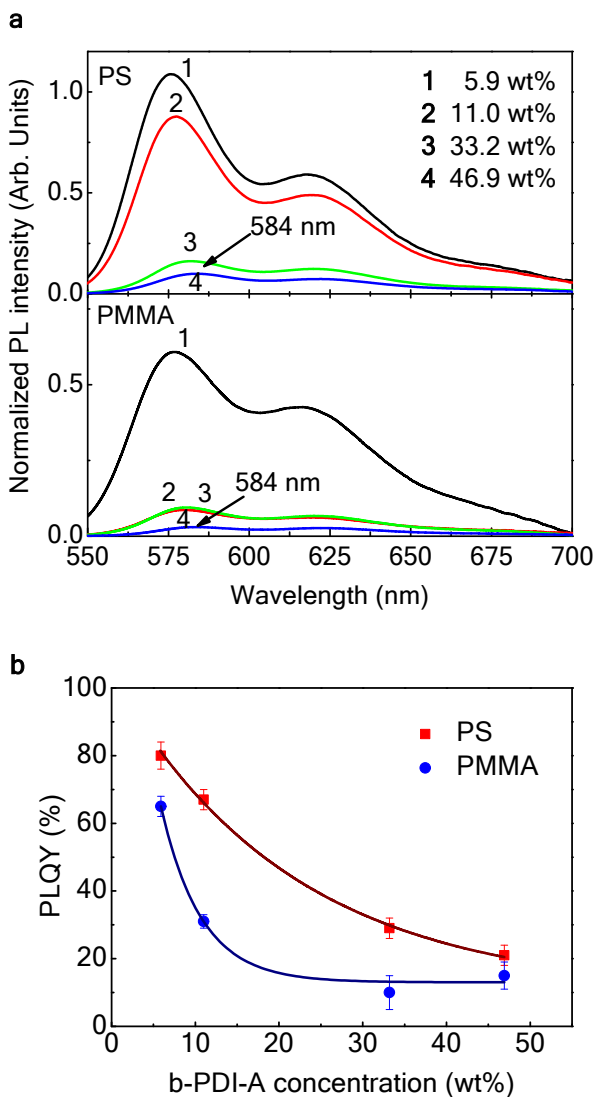
a

b

**Figure 5. Photoluminescence properties of b-PDI-A dispersed in PS and PMMA films.**

Normalized photoluminescence (PL) intensity, i.e. PL intensity divided by the optical density at the excitation wavelength versus wavelength for b-PDI-A dispersed at various doping rates in PS and PMMA films (top and bottom of the panels, respectively). Labels 1, 2, 3 and 4 in the figures correspond to dye concentrations of 5.9, 11, 33.2 and 46.9 wt%, equivalent to 5, 10, 40 and 70 ($\times 10^{-5}$ mol/g). The wavelength of the maximum intensity peak for the film with highest doping rate is indicated next to its corresponding spectrum;

(b) PL quantum yield (PLQY) versus dye concentration for b-PDI-A dispersed in either PS (squares) or PMMA (circles). Full lines are guides to the eye.

ASE properties: spectra, thresholds and operational lifetimes

ASE emission appears at a wavelength (λ_{ASE}) close to the first vibrational PL peak, as it occurs with PDI-O. While ASE emission in the films containing PDI-O occurs at around 580 nm, with b-PDI-A, ASE appears at longer wavelengths, particularly in the range 615-628 nm (see Figure 6a). This is because the PL spectrum is red-shifted with respect to that of PDI-O due to the substituents in the bay positions of the PDI core of b-PDI-A, as already discussed previously.[15] Another important feature is the wide range of emission wavelengths available in this case, which is a consequence of the capacity of this dye to be doped at high rates in the film with no significant PL quenching. The observed shifts for each polymer are in accordance with the shifts observed in the PL peaks.

a

PS

1 2 3 4

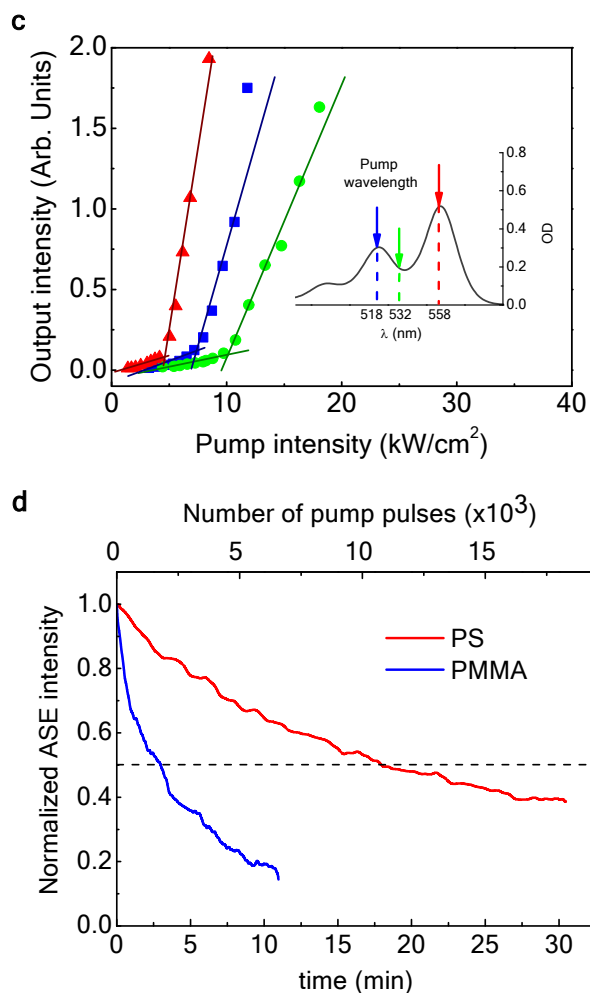| **1** | 5.9 wt% |
2	11.0 wt%
3	33.2 wt%
4	46.9 wt%

PMMA

1 2 3

b

c

d
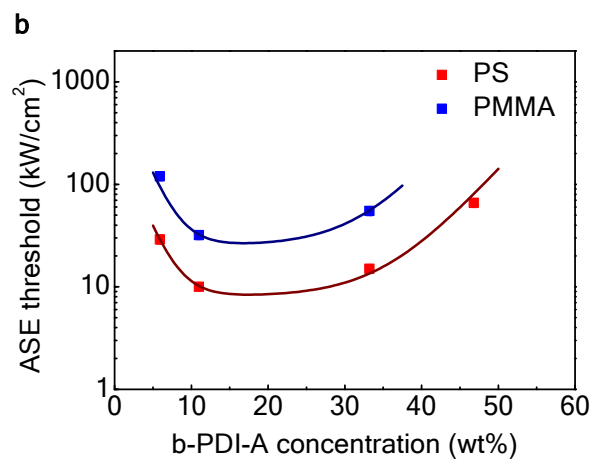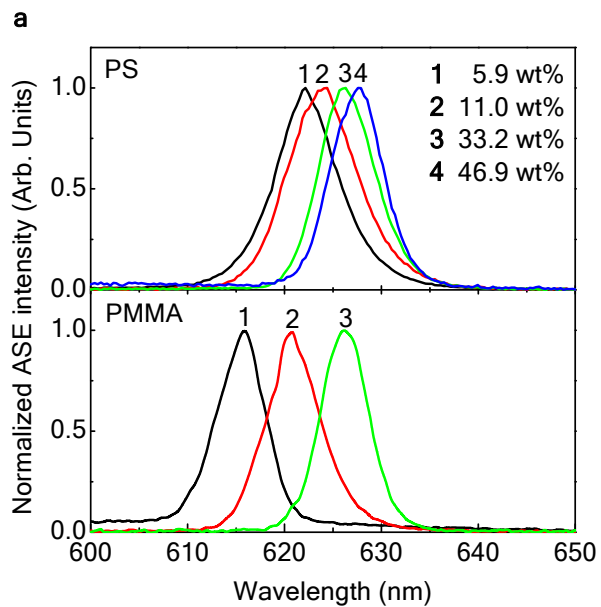
Figure 6. Amplified spontaneous emission (ASE) properties of b-PDI-A dispersed in PS and PMMA films. (a) Normalized ASE spectra, i.e. spectra divided by its maxima for PS and PMMA films (top and bottom of the panel, respectively) doped with b-PDI-A at concentrations of 5.9, 11, 33.2 and 46.9 wt%, equivalent to 5, 10, 40 and 70 ($\times$ 10^{-5} mol/g) (labels 1, 2, 3 and 4, respectively); (b) ASE threshold as a function of dye concentration for PS (squares) and PMMA (circles) films doped with b-PDI-A. The full lines are guides to the eye; (c) Output intensity versus pump intensity for a PS film doped with 11 wt% of b-PDI-A at various pump wavelengths (see inset). Dashed lines are guides to the eye; (d) Normalized ASE intensity at the peak wavelength versus irradiation time (bottom axis) and versus the number of pump pulses (10 ns, 10 Hz; top axis) for films of 11 wt% b-PDI-A

dispersed in PS (red line) and PMMA (blue line) excited at 60 kW/cm^2 (four and two times above their threshold, respectively).

The ASE thresholds for the various films were determined as in the case of PDI-O, i.e. from plots of the FWHM and of the output intensity versus I_{pump}. The obtained $I_{th\text{-}ASE}$ values are represented in Figure 6b as a function of the dye concentration in the films. For both, PS and PMMA, the type of dependence of $I_{th\text{-}ASE}$ on the dye concentration in the film is in agreement with previous results with PS films doped with a similar b-PDI compound:[15] $I_{th\text{-}ASE}$ decreases as the concentration increases, up to a certain concentration (here around 10 wt%), at which the lowest $I_{th\text{-}ASE}$ values are obtained (10 and 32 kW/cm^2 for PS and PMMA films respectively); for higher concentrations, $I_{th\text{-}ASE}$ increases rapidly. As it occurs with PDI-O, at a given concentration, $I_{th\text{-}ASE}$ for PS is in all cases lower than for PMMA, indicating that also for this PDI derivative, the ASE performance, in terms of threshold, is better (lower threshold at a given concentration and larger doping rate at which the ASE threshold starts increasing) in PS than in PMMA.

If we compare the threshold performance of the b-PDI-A-based films (Figure 6b) to that of the PDI-O-based films (Figure 3b), it is seen that the lowest threshold obtained with b-PDI-A ($I_{th\text{-}ASE}$ = 10 kW/cm^2, for the 10 wt% doped PS film) is larger than the one obtained with PDI-O ($I_{th\text{-}ASE}$ = 3 kW/cm^2, for the 1 wt% doped PS film). This difference is somewhat unexpected, taking into account that the PLQY in liquid solution of both PDI derivatives is similar (close to 100%).[4,15] So we considered that this might be because the pump wavelength used in the ASE experiments (λ_{pump} = 532 nm) does not match the absorption

peaks in the case of b-PDI-A. In order to clarify this aspect, we carried out ASE experiments with the best performing b-PDI-A film (the 10 wt% doped PS one) at two additional pump wavelengths, 558 nm and 518 nm, which match the most intense absorption peaks (see Figure 6c). As observed, for $\lambda_{pump} = 558$ nm, at which the absorbance is maximum, $I_{th\text{-}ASE}$ is around 5 kW/cm^2. This value is similar to that obtained for the best-performing PDI-O film (the 1 wt% doped PS one) indicating, that both PDIs behave similarly in terms of threshold whenever the concentration and the pump wavelength are optimized. Importantly, the fact that same threshold can be achieved with both molecules (b-PDI-A and PDI-O) does not mean that they are equally efficient at a molecular level. Note that in order to obtain the optimum threshold, a larger doping ratio (expressed in number of mols of dye per gram of polymer), which implies a larger absorption coefficient at the excitation wavelength, is needed (see data in Table 1, supporting information). This means that at the same concentration (considering the pump wavelength is optimized), PDI-O has a better performance than b-PDI-A, but for practical purposes the same threshold can be achieved with both by properly adjusting the dye content. In any case, the $I_{th\text{-}ASE}$ obtained for b-PDI-A is the lowest reported to date for a b-PDI derivative. This can be considered an excellent result in a general context taking into account that b-PDIs emit in a wavelength range around of 620 nm, which is not accessible by PDI-O or any other PDI derivative with no substitutions at the bay.

The photostability of the b-PDI-A-based films was also investigated. Focusing on the comparison between PS and PMMA, we represent in Figure 6d the evolution of the ASE intensity versus time for the PS and PMMA films with lowest threshold (the ones with 10 wt% of b-PDI-A). The experiments were done at the same pump intensity for both films

(I_{pump} = 60 kW/cm^2), this value being several times above their corresponding ASE thresholds (10 and 32 kW/cm^2, for PS and PMMA, respectively). It is seen that the operational lifetime of the PS film is many times longer than that of PMMA, even at the same pump intensity. Note that the threshold of the PS film is lower, so if the films were pumped at the most possible moderate conditions (i.e. I_{pump} ~ 2 × $I_{th\text{-}ASE}$), the difference between both would be much more significant.

In comparison to PDI-O, the photostability performance of b-PDI-A is inferior, in agreement with the results obtained previously with b-PDI-1 in PS. We are currently working on the design of b-PDIs with improved photostability.

Gain coefficients and propagation losses

Net gain coefficients (g_{net}) and propagation losses for b-PDI-A films were determined following the same method as for PDI-O. The g_{net} values obtained at different I_{pump} values are represented in Figure 7 for the film with lowest threshold (PS with around 10 wt% of b-PDI-A). For PMMA, the photostability was rather poor, so it was not possible to obtain reliable data for the gain and loss coefficients. Nevertheless, according to their thresholds, which are higher than those in PS, they are also expected to be worse. Focusing on the results for PS, in comparison to the best performing PDI-O film (PS with 1 wt %, see Figure 4c), the g_{net} values for b-PDI-A (at similar pump intensities) are somewhat lower, which is in agreement with the threshold results. Nevertheless, as already discussed through the results of Figure 6c, this difference can be eliminated by optimizing the pump wavelength. With respect to the losses, a value of 8 cm^{-1} has been obtained with b-PDI-A, similar to that obtained with the 5 wt% PDI-O film. This indicates that the waveguide quality does not seem to be negatively affected by aggregation effects. In other words, the

variations of threshold and net gain observed upon changing the dye concentration seem to

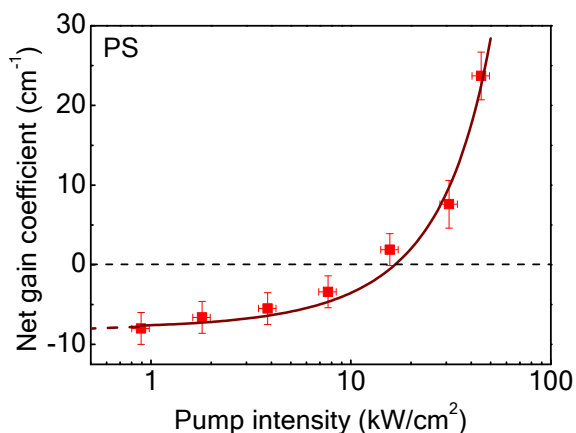be due mainly to changes in PL efficiency rather than in the waveguide losses.

Figure 7. Net gain and loss coefficients of b-PDI-A dispersed in PS films. Net gain

coefficients, obtained from plots such as those of Figure 4a, versus the pump intensity for a

11 wt% b-PDI-A-doped PS film. The full line is a guide to the eye and its intersection with

the Y axis corresponds to the loss coefficient ($k = 8 \pm 1$ cm^{-1}).

Discussion about the different performance of PMMA and PS

Results presented in previous sections indicate that for the two PDI compounds

investigated, PS appears to be a better matrix than PMMA. For both polymers, there are

clear signs (i.e. changes in PL spectral shape, PLQY decrease and ASE threshold increase)

of the existence of processes leading to PL quenching (excimer formation, aggregation,

interaction, etc). We have performed some experiments to characterize film surface using

field-effect scanning electron microscopy (FE-SEM) and confocal microscopy, aiming to

directly see aggregates.[13] The FE-SEM images obtained on samples with different dye

concentrations did not show signs of irregularity or the presence of aggregates or phase

separation. Similarly, preliminary studies with confocal microscopy on samples of both, PS

and PMMA, with low and high dye contents, have not provided useful results: apparently, the fluorescence is uniform across the film and aggregation or phase separation was not observed. Further work with these or other techniques would be needed in order to reach conclusions about the presence of aggregated species. In any case, whatever the type of mechanism responsible for the observation of PL quenching, an important feature is that the dye concentration above which these processes become significant is lower in PMMA than in PS. A possible explanation for this might be based on conformational effects and/or electronic interactions between the dye and the polymer, which depend on the electron-donor character of the substituents. The two PDI derivatives under study present a quite hydrophobic character while the two polymers show certain polarity, which is higher in PMMA than in PS (monomeric dipole moments of 1.67 D and 0.123 D, respectively)[42] as a consequence of the higher electron-donor character of its substituent groups (–COO–, versus phenyl in PS). In previous work dealing with photostability,[4,43] the different electron-donor character of the polymer substituents was used to discuss the photostability performance of PS and PMMA with PDI-O. In those studies, dye photodegradation was attributed to two mechanisms: (i) type II photooxidation, which would predominate under aerobic conditions, and (ii) partially reversible photoreduction, which would prevail under anaerobic conditions. While a key parameter for the first of these mechanisms would be the oxygen permeability of the matrix, the type and strength of the dye–polymer interaction would play a role for the second. Thus, the lower electron-donor character of PS would justify less photoreduction of the PDI-O in PS than in PMMA. On the other hand, oxygen permeability of PMMA is lower than that of PS, so less photooxidation would be expected in the former. Based on this discussion, if the electron-donor character of the polymer substituents seems to play a role in the photodegradation mechanisms, it is reasonable to

31

think that the molecular conformation of the PDIs would be different in PS and in PMMA. Another study that supports the hypothesis of the importance of the electronic interaction between the dye and the polymer is the work of Priimagi et al.[44] They investigated aggregation effects of the polar molecule azo-dye Red 1 in various polymers with different polarity. They found drastic differences among them and concluded that, using the polarity character of the constituents of the film, it is possible to control the amount of aggregation, which plays a very important role in the film optical properties. In order to clarify this issue, further work using a larger set of PDI dyes and host polymers of different polarities is currently underway.

CONCLUSIONS AND PERSPECTIVES

The optical (absorption and photoluminescence, including PLQY), ASE (threshold, operational lifetime and gain) and waveguide losses of films of two polymers widely used in optoelectronic applications - polystyrene (PS) and poly(methyl methacrylate) (PMMA)- hosting two soluble PDI derivatives - PDI-O (commercial derivative) and b-PDI-A (synthesis reported in this work)- have been investigated. The influence on the properties of the dye concentration in the film (up to 8 wt% and 50 wt%, for PDI-O and b-PDI-A, respectively) has been analyzed.

For the PDI-O-based films, PL data, at both room and low temperature, show that the PL vibronic progression is disrupted at lower concentrations in PMMA than in PS, suggesting that the onset of aggregation occurs more easily in the former (2.5 and 5 wt%, for PMMA and PS respectively). The latter is also supported by the observation of a quicker falloff of PLQY for PMMA. For both polymers, the optimal ASE performance is found at low concentrations (1-3 wt% and 1 wt%, for PS and PMMA, respectively) with values slightly

better with PS ($I_{\text{th-ASE}}$ = 3 kW/cm², g_{net} = 38.8 cm⁻¹ at $I_{\text{pump.}}$ = 14.6 kW kW/cm²) in comparison to PMMA ($I_{\text{th-ASE}}$ =12 kW/cm²; g_{net} = 26.8 cm⁻¹, at $I_{\text{pump.}}$ = 19.9 kW/cm²). For larger concentrations the ASE parameters get worse for both polymers, but much quicker upon the dye concentration increase in the case of PMMA. In PS, similar loss coefficients (k = 6-8 cm⁻¹) are found at any concentration between 1 and 5 wt%, indicating that film quality seems not to be affected by the excimer formation. On the other hand, in PMMA the loss, which is larger than in PS, rises significantly (from 15 to 25 cm⁻¹) with increasing concentration within the same range.

For the b-PDI-A-based films, the behavior is similar to that observed with PDI-O in various general aspects: (i) PS is better than PMMA; (ii) there is a dye concentration at which the ASE performance is optimal (in this case 10 wt% and 5 wt%, for PS and PMMA respectively), approximately coincident with the onset concentration at which aggregation appears; (iii) its ASE threshold at the optimal concentration is similar to that of PDI-O whenever the pump wavelength is optimized. On the other hand, distinct features of b-PDI-A with respect to PDI-O are: (i) a much larger dye blending ratio in the film is possible (up to around 50 wt%); (ii) the PL spectral shape does not practically change as the concentration increases (except for a red-shift of the PL peaks), while as it occurs with PDI-O, the PL efficiency decreases with concentration; (iii) ASE emission occurs at longer wavelengths (around 620 nm) with respect to PDI-O (580 nm), and a wider range of wavelengths is possible with b-PDI-A thanks to the larger doping rates available; (iv) the ASE photostability is inferior.

The better properties of both PDIs in PS than in PMMA, apparently due to a better dye dispersion in the former, are most likely due to conformational effects and/or electronic interactions between the dye and the polymer, which depend on the electron-donor

33

character of the substituents. Therefore, although the matrix is meant to be an inert host for the dyes, results indicate that its interaction (conformational and/or electronic) with the dye affects the optical properties. Further work towards a detailed understanding of these processes is of great interest because this would allow to properly choose a matrix for a given dye as to control the macroscopic organization, which is crucial to optimize the performance.

ASSOCIATED CONTENT

Supporting information

Electric field distribution inside the structures and confinement factor calculations. Absorption and low temperature photoluminescence data for films consisting of PDI-O or b-PDI-A dispersed in either PS or PMMA at various concentrations. Example of ASE plots for threshold and gain coefficient determination. ^{1}HNMR and ^{13}CNMR spectra of b-PDI-A in $CDCl_3$. Table with optical and ASE parameters of PDI-O and b-PDI-A-based PS and PMMA films. The Supporting Information is available free of charge on the ACS Publications website at DOI: XXXX/acs.jpcc.XXXXX.

AUTHOR INFORMATION

Corresponding Authors

* (M.A.D.-G.) Email: maria.diaz@ua.es.

* (F.F.-L.) Email: fdofdez@umh.es.

ORCID

Nathalie Zink-Lorre: 0000-0003-3081-995X

Michael J. Gordon: 0000-0003-01239649

Ángela Sastre Santos: 0000-0002-8835-2486

Fernando Fernández-Lázaro: 0000-0002-4598-6024

María A. Díaz-García: 0000-0001-7025-5699

Notes

The authors declare no competing financial interest.

ACKNOWLEDGMENT

REFERENCES

1. Anni, M.; Lattante, S. Organic Lasers: Fundamentals, Developments, and Applications; Pan Stanford Publishing: Singapore, Singapore, 2018.

2. Kuehne, A. J. C.; Gather, M. C. Organic Lasers: Recent Developments on Materials, Device Geometries, and Fabrication Techniques. *Chem. Rev.* **2016**, *21*, 12823-12864.

3. Navarro-Fuster, V.; Calzado, E. M.; Boj, P. G.; Quintana, J. A.; Villalvilla, J. M.; Díaz-García, M. A.; Trabadelo, V.; Juarros, A.; Retolaza, A.; Merino, S. Highly Photostable Organic Distributed Feedback Laser Emitting at 573 nm. *Appl. Phys. Lett*. **2010**, *97*, 171104.

4. Ramírez, M. G.; Morales-Vidal, M.; Navarro-Fuster, V.; Boj, P. G.; Quintana, J. A.; Villalvilla, J. M. Retolaza, A.; Merino, S.; Díaz-García, M. A. Improved Performance of Perylenediimide-based Lasers. *J. Mater. Chem. C* **2013**, *1*, 1182-1191.

5. Morales-Vidal, M.; Boj, P. G.; Villavilla, J. M.; Quintana, J. A.; Yan, Q.; Lin, N.-T.; Zhu, X.; Ruangsupapichat, N.; Casado, J.; Tsuji, H.; et al. Carbon-bridged Oligo(p-henylenevinylene)s for Photostable and Broadly Tunable, Solution-processable Thin Film Organic Lasers. *Nat. Commun.* **2015**, *6*, 8458.

6. Chen, Y.; Li, Z.; Zhang, Z.; Psaltis, D.; Scherer, A. Nanoimprinted Circular Grating Distributed Feedback Dye Laser. *Appl. Phys. Lett*. **2007**, *91*, 051109.

7. Yamashita, K.; Arimatsu, M.; Takayama, M.; Oe, K.; Yanagi, H. Simple Fabrication Technique of Distributed-feedback Polymer Laser by Direct Photonanoimprint Lithography. *Appl. Phys. Lett*. **2008**, *92*, 243306.

8. Ramirez, M. G.; Boj, P. G.; Navarro-Fuster, V.; Vragovic, I.; Villalvilla, J. M.; Alonso, I.; Trabadelo, V.; Merino, S.; Díaz-García, M. A. Efficient Organic Distributed Feedback Lasers with Imprinted Active Films. *Opt. Express* **2011**, *19*, 22443-22454.

9. Calzado, E. M.; Retolaza, A.; Merino, S.; Morales-Vidal, M.; Boj, P. G.; Quintana, J. A.; Villalvilla, J. M.; Díaz-García, M. A. Two-dimensional -Distributed Feedback Lasers with Thermally-nanoimprinted Perylenediimide-containing Films. *Opt. Mater. Express* **2017**, *7*, 1295-1301.

10. García, O.; Garrido, L.; Sastre, R.; Costela, A.; García-Moreno, I. Synthetic Strategies for Hybrid Materials to Improve Properties for Optoelectronic Applications. *Adv. Funct. Mater.* **2008**, *18*, 2017-2025.

11. Cerdán, L.; Costela, A.; Durán-Sampedro, G.; García-Moreno, I.; Calle, M.; Juan-y-Seva, M.; de Abajo J.; Turnbull, G. A. New Perylene-doped Polymeric Thin Films for Efficient and Long-lasting Lasers. *J. Mater. Chem.* **2012**, *22*, 8938-8947.

12. Calzado, E. M.; Ramirez, M. G.; Boj, P. G.; Díaz-García, M. A. Thickness Dependence of Amplified Spontaneous Emission in Low-absorbing Organic Waveguides. *Appl. Opt.* **2012**, *51*, 3287-3293.

13. Anni, M.; Lattante, S. Amplified Spontaneous Emission Optimization in Regioregular Poly(3-hexylthiophene) (rrP3HT):poly(9,9-dioctylfluorene-cobenzothiadiazole) (F8BT) Thin Films through Control of the Morphology. *J. Phys. Chem. C* **2015**, *119*, 21620-21625.

14. Ramírez, M. G.; Jahnke, J. P.; Junk, M. J. N.; Villalvilla, J. M.; ,Boj, P. G.; Quintana, J. A.; Calzado, E. M.; Chmelka, B. F.; Díaz-García, M. A. Improved Amplified Spontaneous Emission of Dye-Doped Functionalized Mesostructured Silica Waveguide Films. *Adv. Optical Mater.* **2015**, *3*, 1454-1461.

15. Ramírez, M. G.; Pla, S.; Boj, P.G.; Villalvilla, J. M.; Quintana, J. A.; Díaz-García, M. A.; Fernández-Lázaro F.; Sastre-Santos, A. 1,7-Bay-substituted Perylenediimide Derivative with Outstanding Laser Performance. *Adv. Optical Mater.* **2013**, *1*, 933-938.

16. Quintana, J. A.; Villalvilla, J. M.; Morales-Vidal, M.; Boj, P. G.; Zhu, X.; Ruangsupapichat, N.; Tsuji, H.; Nakamura, E.; Díaz-García, M. A. An Efficient and Color-Tunable Solution-Processed Organic Thin-Film Laser with a Polymeric Top-Layer Resonator. *Adv. Opt. Mater.* **2017**, 1700238.

17. Morales-Vidal, M.; Boj, P. G.; Quintana, J. A.; Villalvilla, J. M.; Retolaza, A.; Merino, S.; Díaz-García, M. A. Distributed Feedback Lasers Based on Perylenediimide Dyes for Label-free Refractive Index Sensing. *Sens. Actuators, B: Chem.* **2015**, *220*, 1368-1375.

18. Retolaza, A.; Martínez-Perdiguero, J.; Merino, S.; Morales-Vidal, M.; Boj, P. G.; Quintana, J. A.; Villalvilla, J. M.; Díaz-García, M. A. Organic Distributed Feedback Laser for Label-free Biosensing of ErbB2 Protein Biomarker. *Sens. Actuators B: Chem.* **2016**, 223, 261-265.

19. Boj, P. G.; Morales-Vidal, M.; Villalvilla, J. M.; Quintana, J. A.; Marcilla, A.; Díaz-García, M. A. Organic Distributed Feedback Laser to Monitor Solvent Extraction upon Thermal Annealing in Solution-processed Polymer Films. *Sens. Actuators, B: Chem.* **2016**, *232*, 605-610.

20. Calzado, E. M.; Villalvilla, J. M.; Boj, P. G.; Quintana, J. A.; Navarro-Fuster, V.; Retolaza, A.; Merino, S.; Díaz-García, M. A. Influence of the Excitation Area on the Thresholds of Organic Second-order Distributed Feedback Lasers. *Appl. Phys. Lett.* **2012**, *101*, 223303.

21. Lin, M.; Jiménez, A. J.; Burschka, C.; Würthner, F. Bay-substituted Perylene Bisimide Dye with an Undistorted Planar Scaffold and Outstanding Solid State Fluorescence Properties. *Chem. Commun.* **2012**, *48*, 12050-12052.

22. Calzado, E. M.; Villalvilla, J. M.; Boj, P. G.; Quintana, J. A.; Díaz-García, M. A. Concentration Dependence of Amplified Spontaneous Emission in Organic-based Waveguides. *Org. Electron.* **2006**, *7*, 319-329.

23. Calzado, E. M.; Villalvilla, J. M.; Boj, P. G.; Quintana, J. A.; Gómez, R.; Segura, J. L.; Díaz-García, M. A. Amplified Spontaneous Emission in Polymer Films Doped with a Perylenediimide Derivative. *Appl. Opt.* **2007**, *46*, 3836-3842.

24. Navarro-Fuster, V; Calzado, E. M.; Ramírez, M. G.; Boj, P. G.; Henssler, J. T.; Matzger, A. J.; Hernandez, V.; Navarrete, J. T. L.; Díaz-García, M. A. Effect of Ring Fusion on the Amplified Spontaneous Emission Properties of Oligothiophenes. *J. Mater. Chem.* **2009**, *19*, 6556-6567.

25. Lattante, S.; Cretí, A.; Lomascolo, M.; Anni, M. On the Correlation between Morphology and Amplified Spontaneous Emission Properties of a Polymer: Polymer Blend. *Org. Electron.* **2016**, *29*, 44-49.

26. Kazlauskas, K.; Kreiza, G.; Bobrovas, O.; Adomėnienė, O.; Adomėnas, P.; Jankauskas, V.; Juršėnas, S. Fluorene- and Benzofluorene-cored Oligomers as Low Threshold and High Gain Amplifying Media. *Appl. Phys. Lett.* **2015**, *107*, 043301.

27. Al-Kaysi, R. O.; Ahn, T. S.; Müller, A. M.; Bardeen, C. J. The Photophysical Properties of Chromophores at High (100 mM and Above) Concentrations in Polymers and as Neat Solids. *Phys. Chem. Chem. Phys.* **2006**, *8*, 3453-3459.

28. Sheridan, A. K.; Buckley, A. R.; Fox, A. M.; Bacher, A.; Bradley, D.D. C.; Samuel, I. D. W. Efficient Energy Transfer in Organic Thin Films-implications for Organic Lasers. *J. Appl. Phys.* **2002**, *92*, 6367-6371.

29. Calzado, E.M.; Villalvilla, J.M.; Boj, P.G.; Quintana, J.A.; Gómez, R.; Segura, J.L.; Díaz-García, M.A. Effect of Structural Modifications in the Spectral and Laser Properties of Perylenediimide Derivatives. *J. Phys. Chem. C* **2007**, *111*, 13595-13605.

30. Díaz-García, M. A.; Calzado, E.M.; Villalvilla, J.M.; Boj, P.G.; Quintana, J.A.; Céspedes-Guirao, F.J.; Fernández-Lázaro, F.; Sastre-Santos, A. Effect of Structural Modifications in the Laser Properties of Polymer Films Doped with Perylenebisimide Derivatives. *Synth. Met.* **2009**, *159*, 2293-2295.

31. Swanepoel, R. Determination of the Thickness and Optical Constants of Amorphous Silicon. *J. Phys. E.: Sci. Instrum.* **1983**, *16*, 1214-1222.

32. Calzado, E. M.; Villalvilla, J. M.; Boj, P. G.; Quintana, J. A.; Díaz-García, M. A. Tuneability of Amplified Spontaneous Emission through Control of the Thickness in Organic-based Waveguides. *J. Appl. Phys.* **2005**, *97*, 093101.

33. Anni, M.; Perulli, A.; Monti, G. Thickness Dependence of the Amplified Spontaneous Emission Threshold and Operational Stability in Poly(9,9-dioctylfluorene) Active Waveguides. *J. Appl. Phys.* **2012**, *111*, 093109.

34. McGehee, M. D.; Gupta, R.; Veenstra, S.; Miller, E. K.; Díaz-García, M. A.; Heeger, A. J. Amplified Spontaneous Emission From Photopumped Films of a Conjugated Polymer. *Phys. Rev. B* **1998**, *58*, 7035-7039.

35. Cerdán, L.; Costela, A.; Durán-Sampedro, G.; García-Moreno, I. Random Lasing From Sulforhodamine Dye-doped Polymer Films with High Surface Roughness. *Appl. Phys. B* **2012**, *108*, 839-850.

36. Ferreira, J. A.; Porter, G. Concentration Quenching and Excimer Formation by Perylene in Rigid Solutions. *J. Chem. Soc. Faraday Trans. 2* **1977**, *73*, 340-348.

37. Schlosser, M.; Lochbrunner, S. Exciton Migration by Ultrafast Förster Transfer in Highly Doped Matrixes. *J. Phys. Chem. B* **2006**, *110*, 6001-6009.

38. Mikhnenko, O. V.; Cordella, F.; Sieval, A. B.; Hummelen, J. C.; Blom, P. W. M.; Loi, M. A. Temperature Dependence of Exciton Diffusion in Conjugated Polymers. *J. Phys. Chem. B* **2008**, *112*, 11601−11604.

39. Carach, C.; Gordon, M.J. Optical Measures of Thermally Induced Chain Ordering and Oxidative Damage in Polythiophene Films. *J. Phys. Chem. B* **2013**, *117*, 1950-1957.

40. Spano, F. The Spectral Signatures of Frenkel Polarons in H- and J-Aggregates. *Acc. Chem. Res*. **2010**, *43*, 429−439.

41. Zink-Lorre, N.; Font-Sanchis, E.; Sastre-Santos, Á.; Fernández-Lázaro, F. Direct Alkylthio-functionalizacion of Unsubstituted Perylenediimides. *Org. Biomol. Chem.* **2016**, *14*, 9375-9383.

42. Lide, D. R. *CRC Handbook of Chemisty and Physics*; CRC Press: Boca Raton, U. E., 2005.

43. Tanaka, N.; Barashkov, N.; Heath, J.; Sisk, W. Photodegradation of Polymer-dispersed Perylene Di-imide Dyes. *Appl. Opt.* **2006**, *45*, 3846-385.

44. Priimagi, A.; Cattaneo, S.; Ras, R. H. A.; Valkama, S.; Ikkala, O.; Kauranen, M. Polymer-Dye Complexes: a Facile Method for High Doping Level and Aggregation Control of Dye Molecules. *Chem. Mater.* **2005**, *17,* 5798-5802.

1
2
3
4
5
6
7
8
9
10
11
12
13
14
15
16
17
18
19
20
21
22
23
24
25
26
27
28
29
30
31
32
33
34
35
36
37
38
39
40
41
42
43
44
45
46
47
48
49
50
51
52
53
54
55
56
57
58
59
60

FOR TABLE OF CONTENTS ONLY